Microsc. Microanal. Microstruct. 7 (1996) 339–344 OCTOBER/DECEMBER **1996**, PAGE 339

Classification
Physics Abstracts
81.05.Mh — 07.05.Pj

Morphological Segmentation of Cutting Tools

Gervais Gauthier (*), Michel Coster, Liliane Chermant and Jean-Louis Chermant

LERMAT, URA CNRS 1317, ISMRA, 6 bd du Maréchal Juin, 14050 Caen Cedex, France

Résumé. — L'influence de la microstructure des outils de coupe sur leurs propriétés mécaniques est maintenant bien établie. L'étude des caractéristiques de la microstructure nécessite la segmentation des grains de carbure de tungstène dans la phase cobalt. Longtemps, cette segmentation a été effectuée manuellement. Depuis quelques années, le développement des outils de traitement d'image a permis la segmentation automatique d'images de tels matériaux. Une méthode de segmentation de cermets carbure de tungstène-cobalt (WC-Co) est présentée et les résultats obtenus par celle-ci sont comparés à des résultats obtenus par segmentation manuelle afin de valider la méthode.

Abstract. — The influence of microstructural features of cutting tools in tungsten carbide-cobalt cermets (WC-Co) on their mechanical behaviour is well established. The study of these features needs to segment WC grains in the cobalt matrix. This segmentation had been manually performed for a long time, but the development of new image processing tools allow now to automatically achieve a good segmentation. A method of WC-Co segmentation is introduced and the results obtained on this one are compared to the results obtained on a manual segmentation in order to validate the segmentation algorithm.

1. Introduction

Discovered in early twentieth century, the WC-Co cermets had been swiftly used by cutting tool manufacturers because they offer good mechanical properties, such as great hardness and great abrasion strength. These qualities are connected to the intrinsic properties of the WC and Co phases as well as to their microstructure. Previous works have demonstrated the significant influence of microstructural attributes such as the grain size distribution or the mean free path in Co phase on the mechanical behaviour [1-3]. So the analysis of microscopic observation of WC-Co cermets gives precious information for a better knowledge of their mechanical properties. This work is based on the thesis of Gauthier [4].

(*) Now at ADCIS S.A., 7 rue Alfred Kastler, 14000 Caen, France

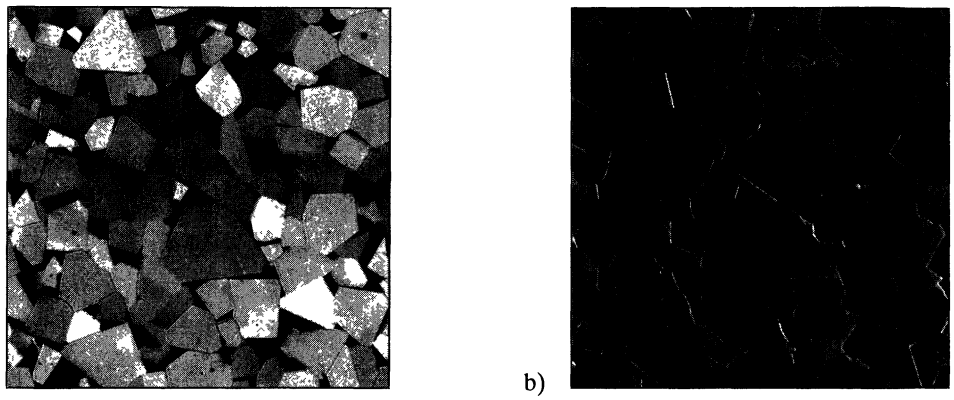

a) b)

Fig. 1. — Etched polished surface of a WC-9.5wt% Co cermet observed in SEM (acceleration: 15 kV) using BSEC mode (a) and BSET mode (b).

2. Materials and Experimental Details

WC carbide crystallizes in the hexagonal system. Its growing is greater in the basal plane than in the prismatic planes. The intersection of a monocrystal by a random plane produces polygonal sections, principally composed by rectangles, triangles and trapezia. Co phase, binder of this hard metal, can be considered as a quasi-continuous framework because the size of its grains is about a few millimeters while the size of WC grains is about a few micrometers.
WC-Co cermets were polished and etched by potassium hydroxide (KOH reagent) in order to reveal the two phases as well as contiguous boundaries of WC grains. Then the samples were examined in a scanning electron microscope (SEM) (Jeol T330) because it offers a suitable spatial resolution for the WC grains analysis, and a multi-modal detection particularly useful to get the complementary information needed to segment grains. In fact, the back scattered electron composition (BSEC) images give significant information on composition and on the boundaries between two WC grains which have different grain orientations thanks to the channelling contrast, while the scattered electron topography (BSET) images principally reveal the etched grain boundaries, marked by high grey levels or low grey levels according to their orientation respectively to the SEM detector (Fig. 1).
The automatic image analysis system used for this work is a Matra Pericolor 3100. Its interface to the SEM Joel T330 had allowed to get enhanced image acquisition thanks to its capability of scanning control.

3. Segmentation

The image contrast between the WC and Co phases is strongly marked in the BSEC images (Fig. 2a) and a threshold could be adequate. But the etched grain boundaries interfere a little bit this segmentation, so a low-pass filtering before the threshold is more advisable. The median filter is the most suitable low-pass filter in this case because it smoothes the flat regions (WC grains and Co phase) while enhances edges (grain boundaries). The automatic contrast-based threshold [5] gets correct segmentation, but the weight interclass standard deviation maximization based threshold [6] (Fig. 2b) gets a more proper segmentation with a less calculation time. Then, a weight interclass standard deviation maximization based threshold is performed (Fig. 2c).
In the BSEC images, the grain boundaries between two adjacent grains which the orientations are different, are revealed by gradient filtering. The external morphological gradient filter

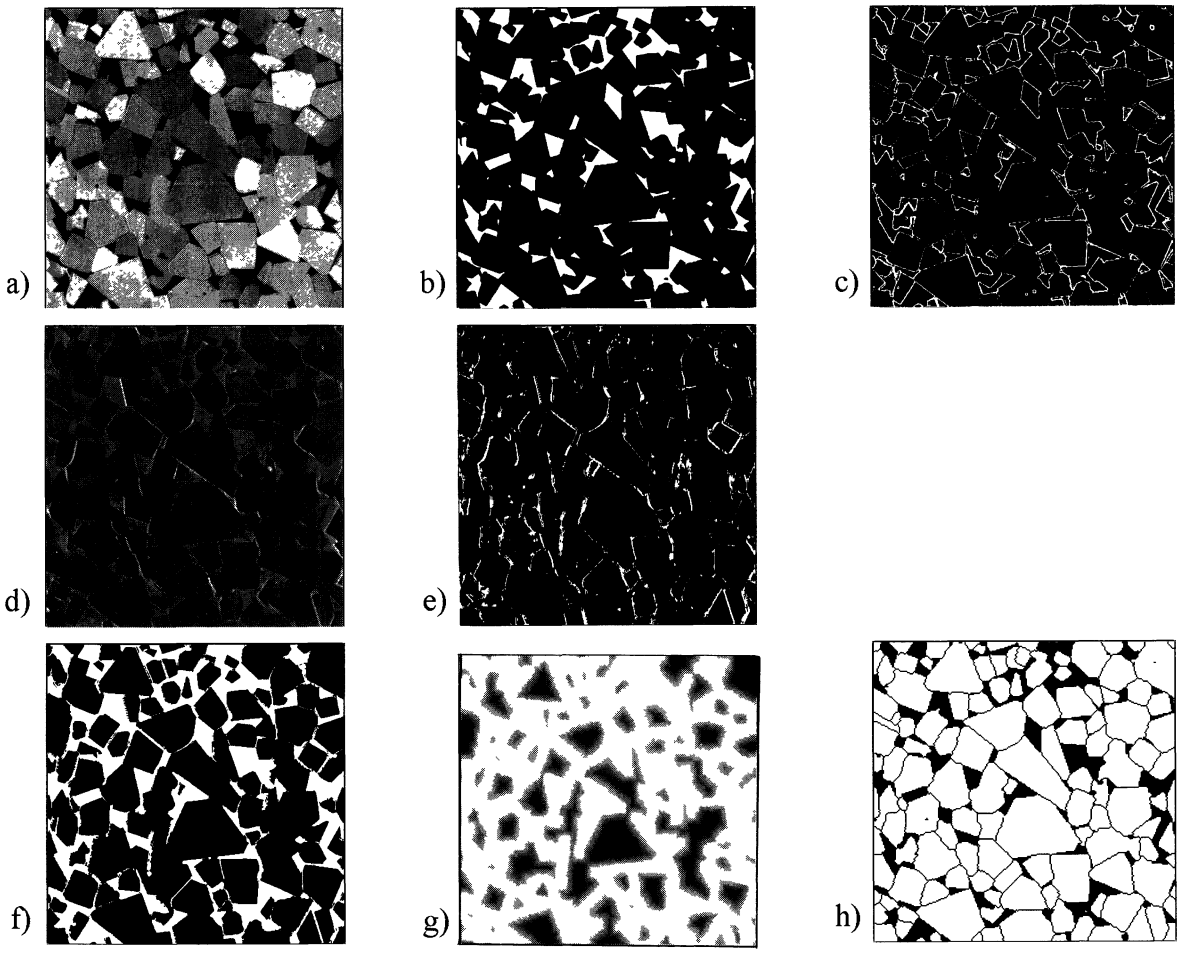

Fig. 2. — BSEC image (a), segmented Co phase (b), edges due to the channelling contrast (c), BSET image (d), combination of white and black top-hats (e), combination of (c) and (e) images (f), complementary image of the WC grain distance image (g), final WC grain segmentation (h).

applied to the BSEC images smoothed by median filtering gets the best results for our series of images (Fig. 2a). In the BSET images, the etched grain boundaries correspond to the highest grey levels and to the lowest grey levels according to the orientation of the edges with respect to the BSE detector (Fig. 2d). In addition, these grain boundaries are somewhat rectilinear. Their detection is computed by oriented top-hat transformations applied to the BSET images previously smoothed by morphological openings or closings by perpendicular oriented structuring element. Then, an entropy maximization based threshold is performed (Fig. 2e).

A combination of the three binary images, *i.e.* the segmented cobalt phase, the edges segmented from the BSEC image due to the channelling contrast and the etched grain boundaries segmented from the BSET image, is computed (Fig. 2f).

At this step, some grain boundaries are not completely segmented. So, the propagation algorithm proposed by Kurdy [7] is used in order to connect the partially segmented grain boundaries. A few grain boundaries are enough segmented because they had been revealed neither by channelling contrast nor by etching. However, the most part of them can be obtained thanks

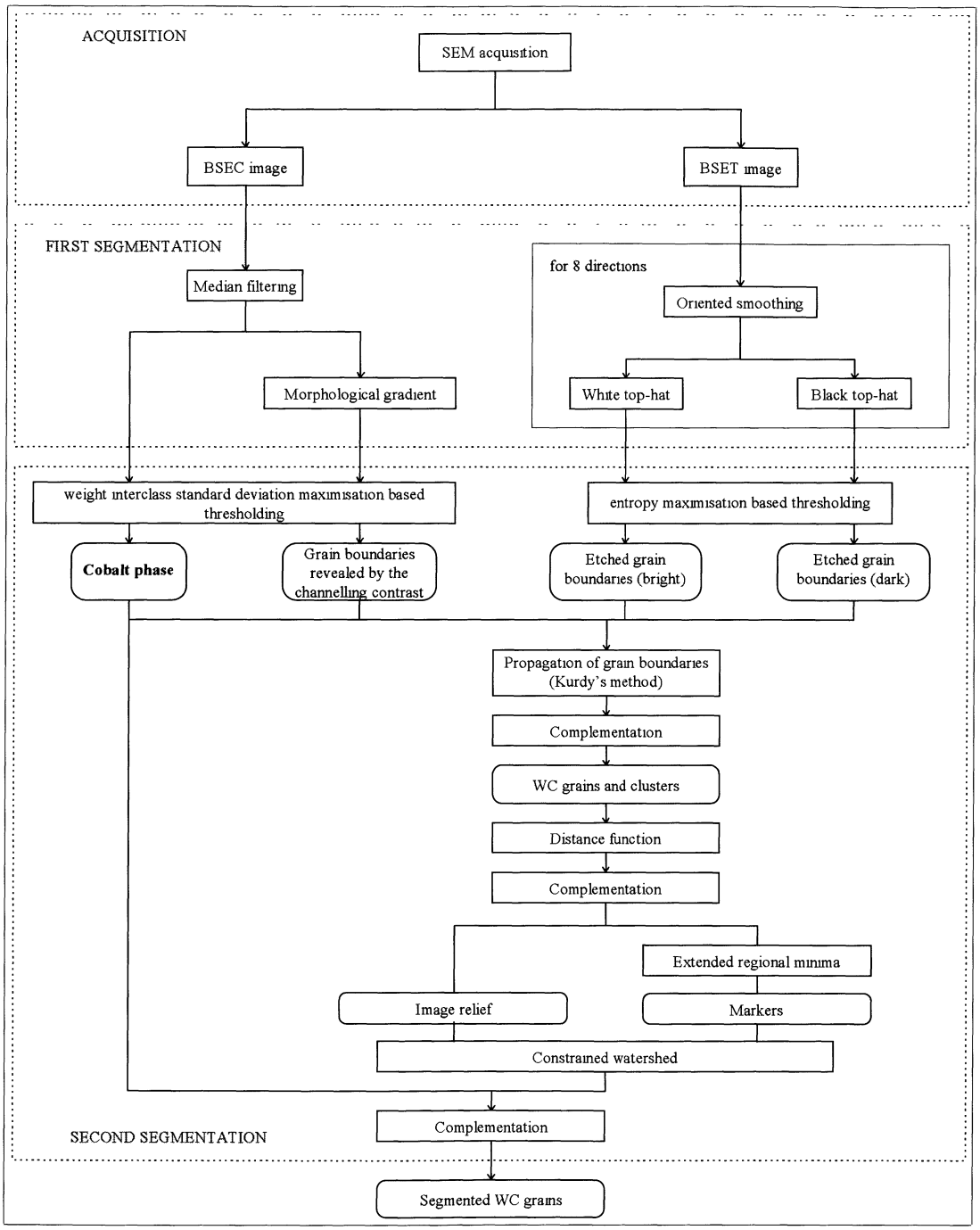

Fig. 3. — Graph of WC-Co segmentation algorithm.

Table I. — *Comparison of morphological characteristics calculated on the automatically segmented images and on the manually segmented images. Variation is a difference between the measurements from automatically segmented image and from manually segmented image.*

	automatic segmentation	intermediate manual segmentation (step 1)	manual segmentation (steps 1 and 2)
S_V(WC/WC)	324 mm^{-1}	303 mm^{-1}	334 $mm^{-1} \pm 40$
variation	−3%		
C(WC/WC)	0.332	0.325	0.335 ± 0.011
variation	−1%		
N_A(WC)	24 414 mm^{-2}	21 362 mm^2	24 976 $mm^{-2} \pm 3\,750$
variation	−2.2%		
D(WC)	5.56 μm	5.87 μm	5.51 μm
variation	< 1%		
σ (D_{WC})	3.10 μm	3.24 μm	3.01 μm
variation	3%		

to the following hypothesis based on a physical property of this material: the WC grains are convex. In fact, all the connected regions which are convex are grains while these ones are not convex are clusters of grains. The method that we propose to segment the clusters is the following: computation of the distance function on the current segmentation of WC grains (composed of grains and clusters), inversion of the resulting image, computation of the extended regional minima (using h-concave transformation [8]), and computation of a constrained watershed using the extended regional minima as markers. The result is shown in Figure 2h.
The graph in Figure 3 summarize the proposed algorithm.

4. Morphological Characteristics

The purpose of the previously presented segmentation is to be able to calculate the morphological characteristics of the microstructure. Thanks to the segmentation of the two phases, the following characteristics can be computed:

- V_V(Co), the cobalt volume fraction,
- V_V(WC), the tungsten carbide volume fraction,
- S_V(WC/Co), the WC-Co interface area per unit volume.

Other characteristics can only be calculated on the complete segmentation (see Tab. I) such as:

- S_V(WC/WC), the WC grain boundary specific surface area per unit volume,
- N_A(WC), the number of WC grains per unit volume,
- Contiguity, $C(\mathrm{WC/WC}) = \dfrac{S_V(\mathrm{WC/WC})}{(\mathrm{WC/Co}) + 2S_V(\mathrm{WC/WC})}$,
- WC grain size distribution.

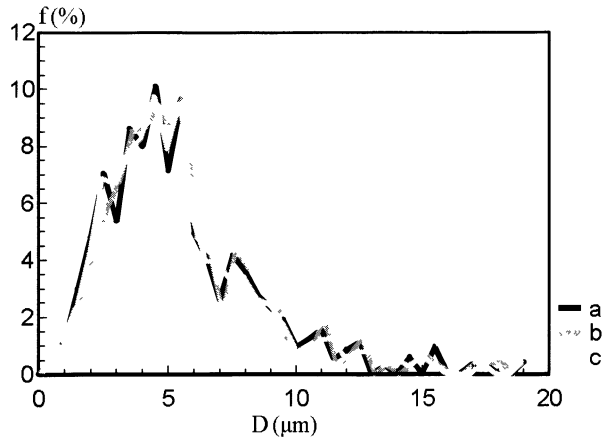

Fig. 4. — WC grain size distribution obtained by automatic segmentation (a) followed by the removal of the wrong grain boundaries (b) and the addition of the missing grain boundaries (c) by an expert.

5. Results and Conclusion

In order to validate the proposed automatic segmentation, we have compared the morphological characteristics calculated on the automatic segmented images and these ones calculated on the corresponding manually segmented images.
The manual editing of the WC-Co segmentation is a drudgery, so the segmentation by an expert was executed in correcting the result of the automatic segmentation previously described. This correction was done in two steps: a) removal of the wrong grain boundaries, b) addition of the missing grain boundaries.
Table I and Figure 3 show the results obtained from the three kinds of segmentation and their comparison.
We note that the results obtained from the automatic segmentation are enclosed by the results obtained from the "under segmented" images and these ones obtained from the "over segmented" images. In addition, the measurement variation calculated on the manually segmented images is higher than the variation between the results got from the automatically and the manually segmented images. So, the results are satisfactory and the proposed automatic segmentation method is convincing.

References

[1] Gurland J., *Powd. Met.* **4** (1961) 221.
[2] Chermant J.L., Deschanvres A. and Osterstock F., *Powd. Met.* **20** (1977), 63.
[3] Chermant J.L. and Osterstock F., *J. Mat. Sci.* **11** (1976) 1939.
[4] Gauthier G., Applications de la morphologie mathématique fonctionnelle : Analyse des textures en niveaux de gris et segmentation par approche multimodale, Thèse de Doctorat de l'Université de Caen (1995).
[5] Kohler R., *Comput. Graph. Image Proc.* **15** (1981) 319.
[6] Zeboudj J.R., Filtrage, seuillage automatique, contraste et contours : du pré-traitement à l'analyse d'image, Thèse de Doctorat de l'Université de Saint-Étienne (1988).
[7] Kurdy M.B. and Jeulin D., *Acta Stereol.* **8** (1989) 473.
[8] Grimaud M., La géodésie numérique en morphologie mathématique. Application à la détection automatique de microcalcifications en mammographie numérique, Thèse de Doctorat de l'École Nationale Supérieure des Mines de Paris (1991).